

# Conservation Properties in the Time-Dependent Hartree Fock Theory

Lu Guo\*,<sup>1</sup> J. A. Maruhn,<sup>1</sup> P.-G. Reinhard,<sup>2</sup> and Y. Hashimoto<sup>3</sup>

<sup>1</sup>*Institut für Theoretische Physik, Universität Frankfurt, 60438 Frankfurt, Germany*

<sup>2</sup>*Institut für Theoretische Physik II, Universität Erlangen-Nürnberg, 91058 Erlangen, Germany*

<sup>3</sup>*Graduate School of Pure and Applied Sciences, University of Tsukuba, Tsukuba 305-8571, Japan*

We discuss the conservation of angular momentum in nuclear time-dependent Hartree-Fock calculations for a numerical representation of wave functions and potentials on a three-dimensional cartesian grid. Free rotation of a deformed nucleus performs extremely well even for relatively coarse spatial grids. Heavy ion collisions produce a highly excited compound system associated with substantial nucleon emission. These emitted nucleons reach the bounds of the numerical box which leads to a decrease of angular momentum. We discuss strategies to distinguish the physically justified loss from numerical artifacts.

PACS numbers: 21.60.Jz, 25.70.-z

Time-dependent Hartree-Fock (TDHF), originally proposed by Dirac [1], has found widespread applications in various areas of physics due to the overwhelming development of computational power. It is employed, e.g., as the variant time-dependent density functional theory [2] in atomic, molecular and cluster physics, see e.g. [3, 4]. It has enjoyed application in nuclear dynamics since more than thirty years [5] as a microscopic approach to various dynamical scenarios in the regime of large amplitude collective motion, like fusion excitation functions, fission, deep-inelastic scattering, and collective excitations; for early reviews see, e.g., [6, 7]. With the steady upgrade of computational power, three-dimensional TDHF calculations without any symmetry restriction became possible and renewed the interest in nuclear TDHF as seen from an impressive series of recent publications [8, 9, 10, 11, 12, 13, 14, 15, 16, 17]. A crucial aspect in nuclear TDHF is that nuclei are freely moving objects such that all conservation laws (energy, momentum, angular momentum) apply. Conservation of energy and momentum is a basic feature which has been tested for all existing codes. Conservation of angular momentum has not yet been studied and that is the topic which we want to address in this paper.

The calculations employ grids in coordinate space. Their finite spacing and box size destroy translational and rotational symmetry which, in turn, can spoil conservation of momentum and angular momentum. The major destructive mechanism comes from matter which tries to leave the computational box but is hindered by the boundary condition. In the course of time development, higher energy components appear in the nucleon wave functions, representing outgoing “particles” from the nucleus. The further time development may therefore be affected by their reflection from the boundary or, in the case of periodic boundary conditions, re-entry from the neighboring cells. That can change the total angular

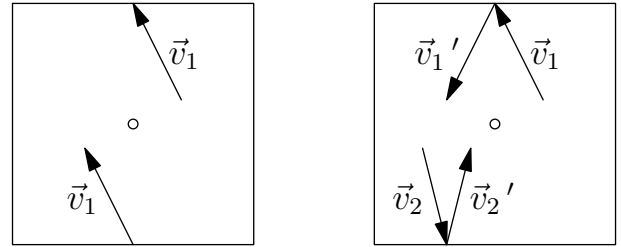


FIG. 1: Simple illustration of the effect of boundary conditions on total angular momentum. The boxes indicate the computational boundaries and the central dot the reference point for the angular momentum. For periodic boundary conditions (left) it is easy to even revert the sign of the particle’s angular momentum. For approximately reflecting boundary conditions (right) the situation is not quite as pronounced: for the case  $\vec{v}_1$  there is no change by reflection, while for  $\vec{v}_2$  the sign also changes.

momentum, as is illustrated in Fig. 1. Clearly the boundary can even change the sign of a particle’s contribution to the angular momentum around the center of the cell. In this work we consider periodic boundary conditions. The case of reflecting boundaries behaves qualitatively similar.

The static and time-dependent Hartree-Fock equations are solved on a cartesian three-dimensional mesh without any symmetry requirements. The grid spacing was 1 fm, and the Skyrme energy functional [18] was employed with the parametrization SLy6 [19] (for the purposes of this work, the particular choice of Skyrme force is irrelevant). The minimum set of time-odd terms to assure Galilei invariance [18, 20, 21] was included. The spatial derivatives are calculated using the Fast Fourier Transform and periodic boundary conditions are employed, except for the Coulomb potential, which is calculated with boundary conditions at infinity as described in [22]. The time stepping employs a sixth-order Taylor expansion of the time evolution operator  $U(t, t + \Delta t) = \exp[-ih(t + \Delta t/2)\Delta t/\hbar]$ , with the mean fields at the half step estimated by a third-order expansion using the

\*Present address: Department of Physics, University of Tokyo, Hongo, Tokyo 113-0033, Japan

mean field at time  $t$ .

This method of time development is non-unitary, so that the orthonormality of the single-particle wave functions is not guaranteed. Nevertheless, we find that the calculation is quite stable and accurate for several thousand time steps  $\Delta t \approx 0.2 \text{ fm}/c$ , in the sense that the particle number changes by less than 0.1%. The total energy also is conserved to a fraction of an MeV. When instability then sets in, there is a rapid drift of particle number and energy, so that the conservation properties are quite good checks for the accuracy and stability of the calculation.

Test case will be a collision of two  $^{16}\text{O}$  nuclei which involves truly large amplitudes and carries a large amount of excitation energy. As argued above, the boundaries of the numerical grid influence the conservation laws. In order to disentangle its effects, we consider three different setups:

1. A small grid with  $24 \times 32 \times 32 \text{ fm}^3$ .
2. A doubled grid of  $48 \times 64 \times 64 \text{ fm}^3$ , so that the collision is surrounded more generously by empty space. Observables are summed over only the smaller grid of case (1), which allows to distinguish the exact physical loss from the artifacts of the smaller grid.
3. Finally, the small grid plus an absorbing boundary conditions which are arranged within an absorbing layer  $N_{\text{abs}} = 6$  cells wide in each direction. In this layer, a mask function  $M(n_x, n_y, n_z) = M_x(n_x)M_y(n_y)M_z(n_z)$  is applied to the wave functions after each time step where  $M_i(n_i) = \cos((N_{\text{abs}} + 1 - n_i)\pi/2N_{\text{abs}})^{0.25}$ ,  $n_i = 1 \dots N_{\text{abs}}$ . See [23] for details.

Before analyzing rotational motion, we have checked, of course the conservation of energy and total momentum. Both quantities are conserved very well with relative fluctuations staying at the order of  $10^{-4}$ . A detailed analysis of translational motion and of the physical interpretation of the TDHF single-particle energies can be found in [17]. Let us just mention here that for a nucleus moving freely in any direction on the grid the momentum is conserved to an accuracy of better than  $10^{-4}$ .

For the case of angular momentum, the situation turned out to depend strongly on the excitation of the system. We therefore discuss two types of calculations: single cranked nucleus and heavy-ion collisions.

### A. Single cranked nucleus

We produce a rotating nucleus by solving the cranked static Hartree-Fock equations

$$(\hat{h} - \omega \hat{J}_x) \phi_k(\vec{r}) = \varepsilon_k \phi_k(\vec{r}), \quad k = 1 \dots A \quad (1)$$

with  $\omega$  the prescribed angular frequency of rotation about the  $x$ -axis (for simplicity we omit spin dependence,

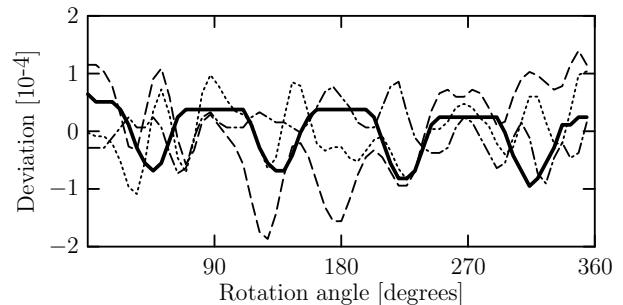


FIG. 2: Relative deviations of the angular momentum expectation value (full curve) and the three principal moments of inertia (smallest: dotted, intermediate: dashed, and  $i$  largest: dot-dashed curve) from the temporal average during rotation of a  $^{24}\text{Mg}$  nucleus. The abscissa denotes the rotation angle calculated from the instantaneous tensor of inertia.

though spin is included in the calculations). The rotating states

$$\bar{\phi}_k(\vec{r}, t) = \exp\left[-\frac{i\omega t \hat{J}_x}{\hbar}\right] \exp\left[-\frac{i\varepsilon_k t}{\hbar}\right] \phi_k(\vec{r}) \quad (2)$$

then are exact solutions of the TDHF equations, so that the numerical solution should show simply a rotating nucleus with no extraneous motion added.

It is clear that this is a much more demanding test for the numerical solution, since the cartesian grid is incompatible with rotational motion and effectively the grid spacing expands and shrinks by a factor of  $\sqrt{2}$  as the nucleus rotates through 45 and then 90 degrees.

As an example, we show here the deformed nucleus  $^{24}\text{Mg}$  cranked with  $\omega = 2 \text{ MeV}/\hbar$ . In this case, rotation turns out to be almost completely of rigid-body type; the observed angular momentum of  $7.54 \hbar$  corresponds to a moment of inertia of about 98% of the rigid-body value. To judge the accuracy of the rotation in the numerical solution, we examine the expectation value of the angular momentum  $\hat{J}_x$ , which should be strictly conserved, and the principal moments of inertia, which in the absence of any internal excitation should also be constant. Fig. 2 shows the fluctuations of these quantities as functions of simulation time.

The most striking result is the excellent quantitative description of rotation in spite of the coarse Cartesian grid, the variations being of the order of  $10^{-4}$ . The angular-momentum expectation value clearly is correlated with the angle and shows regular variations with a 45 structure. The variations in the moments of inertia show a less regular pattern and appear to be influenced by the periods of the internal vibrations of the nucleus from which seemingly a tiny amount is exited during the rough sliding over the grid.

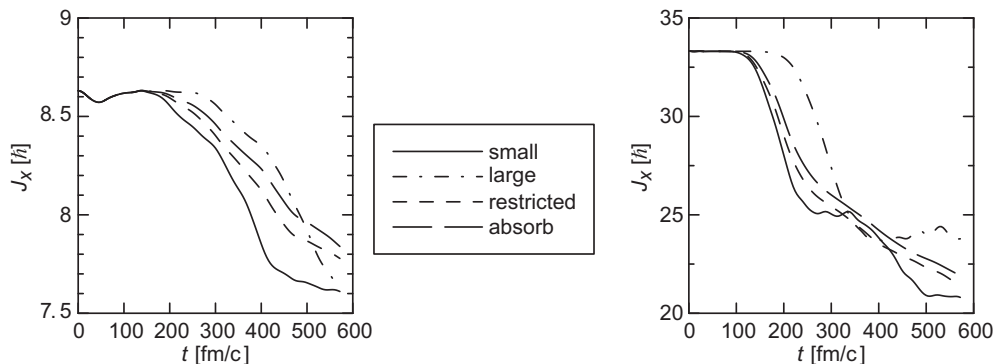


FIG. 3: Angular momentum as a function of time for collisions of  $^{16}\text{O}+^{16}\text{O}$  at  $E_{\text{cm}} = 25$  MeV (left) and 125 MeV (right). The different cases are: “small”: calculation in a grid of  $24 \times 32 \times 32 \text{ fm}^3$ , “large”: calculation in a grid doubled in total size in every direction, “restricted”: same as large, but angular momentum is summed up only over the small grid; “absorb”: small grid with a 6 fm absorbing layer around the boundary.

### B. Heavy-ion reactions

The situation is quite different in the more violent case of heavy-ion collisions. The substantial excitation leads to emission of nucleons which, in turn, causes problems. As was shown in the introduction, particles crossing the boundaries can generate large spurious changes in the total angular momentum and it becomes quite difficult to separate the correct physical loss of angular momentum carried away by the emitted particles from the spurious numerical effect. The results presented in Fig. 3 illustrate the problems which are of quite general nature. Note that the angular momentum  $J_x$  is perpendicular to the reaction plane.

The initial condition consists of two ground-state  $^{16}\text{O}$  nuclei with a c.m. energy of either 25 or 125 MeV. All the initial angular momentum thus comes from the relative motion. For the higher energy the impact parameter was  $b = 4.8$  fm, corresponding to  $J_x \approx 33\hbar$ , while for the lower energy  $b = 2.8$  fm corresponding to  $J_x \approx 8.6\hbar$ . These values were chosen to have the same distance of closest approach in the pure Coulomb trajectory.

For both energies, the two nuclei stay fused at the end of the calculation. The boundary problems are more serious for the higher energy because of the higher excitation leading to stronger emission of particles. It is apparent that in the larger grid the reduction in angular momentum starts about 100 fm/c later as compared to the small grid. The curve labeled “restricted” is computed in the large grid while the angular momentum is collected in the small grid. This should indicate the true loss of angular momentum from the small grid for the time span before emitted particles come back from the larger boundary. Clearly the “small” calculation has the largest loss and it becomes even unreasonable at about 250 fm/c. It is reassuring that the curve for the absorbing boundary stays quite close to the “restricted” calculation and shows a reasonable monotonic decrease throughout.

The total reduction of about 30% at a collision energy of 125 MeV is surprisingly large in view of the fact

that only 1.7 nucleons are absorbed. These nucleons thus carry a comparatively large share of angular momentum. At the lower energy of 25 MeV, the total change in angular momentum is not as dramatic but by no means negligible, still exceeding 10% while 0.4 nucleons are emitted. Besides the quantitative difference, the general pattern are very similar. Again, the loss sets in later for the larger grid and the calculation with the absorbing layer appears to be a reasonable approximation to the “true” loss.

In this paper, we have analyzed the conservation of total angular momentum in nuclear TDHF calculations. The calculations used a coordinate-space representation of wave functions and potential fields on a three-dimensional cartesian grid without any symmetry restriction. The full Skyrme interaction was taken into account. Conservation of energy and momentum was tested (but not detailed here) and found to be well matched within a relative error of only  $10^{-4}$ .

The results for angular momentum depend on the dynamical scenario. Free rotation of a deformed nucleus is surprisingly well described. Although the cartesian grid spoils rotational symmetry, we find that the deformed nucleus rotates steadily over the grid of 1 fm spacing with variations of angular momentum and moments of inertia of the order of  $10^{-4}$ . This is the same quality as found already for translational momentum and energy.

The case of nucleus-nucleus collisions is less well-behaved. The compound system is heavily excited. This leads to substantial emission of nucleons which in the sequel reach the bounds of the numerical box where reflection or periodic copy (depending in the grid model) lead to a substantial reduction of angular momentum. Comparing calculations on different grids (small box, large box, absorbing bounds), we have worked out that the loss is to a large extent physical because the emitted nucleons are very energetic and carry away a comparatively large amount of angular momentum. Artifacts from the boundary come into play as soon as nucleons travel back into the reaction zone. This happens the later the larger

the grid and it can be effectively avoided when using absorbing boundary conditions. Both “solutions”, larger or absorbing grid are somewhat expensive. One may live with a small grid if one confines the analysis to the early time evolution of the compound system (to evaluate the doorway effects). In any case, the conserved quantities should be checked carefully for each new dynamical scenario.

The results discussed here are, of course, only indicative and may vary quantitatively for other TDHF codes.

The specific discretization of the equations of motion will affect the accuracy of describing an isolated rotating nucleus, while the treatment of the boundary conditions will strongly influence the boundary problems addressed above.

Lu Guo acknowledges support from the Alexander von Humboldt Foundation. We gratefully acknowledge support by the Frankfurt Center for Scientific Computing and from the BMBF (contracts 06 ER 124 and 06 F 131).

- 
- [1] P. A. M. Dirac, Proc. Camb. Phil. Soc. **26**, 376 (1930).
  - [2] E. K. U. Gross and W. Kohn, Adv. Quant. Chem. **21**, 255 (1990).
  - [3] P.-G. Reinhard and E. Suraud, *Introduction to Cluster Dynamics* (Wiley-VCH, Weinheim, 2004).
  - [4] in *Time-dependent density functional theory*, edited by M. A. L. Marques, C. A. Ullrich, and F. Nogueira (Springer, Berlin, 2006), vol. 706 of *Lecture Notes in Physics*.
  - [5] P. Bonche, S. E. Koonin, and J. W. Negele, Phys. Rev. C **13**, 1226 (1976).
  - [6] W. Negele, Rev. Mod. Phys. **54**, 913 (1982).
  - [7] K. T. R. Davies, K. R. S. Devi, S. E. Koonin, and M. R. Strayer, in *Treatise on Heavy Ion Science*, edited by D. A. Bromley (Plenum, New York, 1985), vol. 3, p. 3.
  - [8] C. Simenel and P. Chomaz, Phys. Rev. C **68**, 024302 (2003).
  - [9] C. Simenel, P. Chomaz, and G. de France, Phys. Rev. Lett. **10**, 102701 (2004).
  - [10] T. Nakatsukasa and K. Yabana, Phys. Rev. C **71**, 024301 (2005).
  - [11] A. S. Umar and V. E. Oberacker, Phys. Rev. C **71**, 034314 (2005).
  - [12] J. A. Maruhn, P.-G. Reinhard, P. D. Stevenson, J. R. Stone, and M. R. Strayer, Phys. Rev. C **71**, 064328 (2005).
  - [13] J. A. Maruhn, P.-G. Reinhard, P. D. Stevenson, and M. R. Strayer, Phys. Rev. C **74**, 027601 (2006).
  - [14] A. S. Umar and V. E. Oberacker, Phys. Rev. C **73**, 054607 (2006).
  - [15] A. S. Umar and V. E. Oberacker, Phys. Rev. C **74**, 024606 (2006).
  - [16] P.-G. Reinhard, L. Guo, and J. A. Maruhn, Eur. Phys. J. A **32**, 19 (2007).
  - [17] L. Guo, J. A. Maruhn, and P.-G. Reinhard, Phys. Rev. C **76**, 014601 (2007).
  - [18] M. Bender, P.-H. Heenen, and P.-G. Reinhard, Rev. Mod. Phys. **75**, 121 (2003).
  - [19] E. Chabanat, E. P. Bonche, P. Haensel, J. Meyer, and R. Schaeffer, Nucl. Phys. A **635**, 231 (1998).
  - [20] J. Dobaczewski and J. Dudek, Phys. Rev. C **52**, 1827 (1995).
  - [21] Y. M. Engel, D. M. Brink, K. Goeke, S. J. Krieger, and D. Vautherin, Nucl. Phys. A **249**, 215 (1975).
  - [22] J. W. Eastwood and D. R. K. Brownrigg, J. Comp. Phys. **32**, 24 (1979).
  - [23] P.-G. Reinhard, P. D. Stevenson, D. Almeded, J. A. Maruhn, and M. R. Strayer, Phys. Rev. E **73**, 036709 (2006).